Transient Electrical Birefringence Characterization of Heavy Meromyosin†

Stefan Highsmith*
Department of Biochemistry, School of Dentistry, University of the Pacific, San Francisco, California 94115
Don Eden
Department of Chemistry, San Francisco State University, San Francisco, California 94132
Received December 13, 1984

ABSTRACT: Heavy meromyosin (HMM) and myosin subfragment 1 (S1) were prepared from myosin by using low concentrations of α-chymotrypsin. The light chain distribution in HMM was identical with that of myosin, within experimental error, when analyzed on 12% polyacrylamide gels after electrophoresis. Specific birefringences and birefringence decay times were measured by transient electrical birefringence in 5 mM KCl, 5 mM tris(hydroxymethyl)aminomethane (pH 7), and 1 mM $MgCl_2$ at 4 °C under gentle conditions that reduced the CaATPase activity by less than 10%. For solutions of HMM, by use of electric field pulses shorter than 0.5 μs, the birefringence decay signal from the S1 portions of HMM could be resolved and the rotational motions of the S1 moieties observed directly. The rotation relaxation time, adjusted to 20 °C, was 0.34 μs; this is in quantitative agreement with previous hydrodynamic results obtained by using covalently attached probes. The assignment of the fast decay time obtained with HMM to the S1 portions was confirmed by birefringence decay measurements on free S1, for which the relaxation time was 0.13 μs, corrected to 20 °C. The specific birefringences for S1 and HMM, respectively, were 0.37×10^{-6} and 12.8×10^{-6} (cm/statvolt)^2. Thus, for much longer electric field pulses, the signal from HMM is due almost entirely to its subfragment 2 (S2) portion, and its rotational dynamics can also be monitored directly by using electrical birefringence. The decay of the signal from the S2 portion could be adequately fit without evoking bending of the S2 portion of HMM other than at its junction with S1.

The mechanical properties of the molecules myosin and actin are of interest because in all types of muscle and in many nonmuscle cases these molecules interact with one another and MgATP to do mechanical work. As a result of this interest, the physical properties of myosin and actin have been investigated by using various techniques in many laboratories. Although it is actomyosin that transduces the chemical energy of ATP hydrolysis into work, it appears that it is myosin that moves in the process.

Myosin (Figure 1) is composed of two heavy chains (M_r 230K) and four light chains [M_r 16K, 18K (2), and 20K] (Harrington & Rodgers, 1984). The rod portion in myosin is about 150 nm long (Slater & Lowey, 1967; Elliot & Offer, 1978) and can be readily proteolyzed at a specific location near the globular subfragment 1 (S1)[1] portion (Gergley, 1950; Szent-Gyorgi, 1953; Lowey, 1971; Weeds & Pope, 1977) or over a substantial range near the center of the rod (Lowey, 1971; Sutoh et al., 1978; King, 1976) to produce heavy meromyosin (HMM) and light meromyosin (LMM). The lengths of the LMM and subfragment 2 (S2) portions (see Figure 1) of the rod in myosin are typically 80 and 70 nm, respectively, but the length of S2 in HMM, or when isolated, varies depending on the preparation (Burke et al., 1973; Goodno et al., 1976; King, 1976; Highsmith et al., 1977, 1978; Sutoh et al., 1978).

The crucial mechanical properties required by the mechanism of the prevalent working hypothesis for force generation (Huxley, 1969; Huxley & Simmons, 1971) are flexibility in the myosin molecule at the two proteolytically susceptible locations that are usually called the swivel and the hinge. It is widely accepted that the swivel is a flexible region. Early results from electron microscopy (Lowey, 1971) and proteolytic susceptibility (Gergely, 1950; Szent-Gyorgi, 1953) suggested the region between the S1 and rod portions of myosin is flexible. Later, observations of the hydrodynamic manifestations of segmental motions were first made by using the techniques of fluorescence anisotropy decay (Mendelson et al., 1973) and confirmed by using saturation-transfer electron-spin resonance (Thomas et al., 1975). These results also were confirmed semiquantitatively by transient electrical birefringence measurements (Kobayasi & Totsuka, 1975), but the available instrumentation was incapable of accurately monitoring the fast rotational motions of S1 free or as part of HMM. The hinge region is also thought to be flexible, on the basis of proteolytic susceptibility (Lowey et al., 1969), the ease of thermally induced melting (Burke et al., 1973; Goodno et al., 1976) in that region, and the observation of bends in myosin electron micrographs (Lowey, 1971; Takahashi, 1978; Eliot & Offer, 1978). More direct hydrodynamic measurements of transient electrical birefringence (Highsmith et al., 1977; Bernengo & Cardinand, 1982) and light scattering (Highsmith et al., 1982) indicated the hinge region is flexible, although there are indications that there may also be a substantial restoring force to the bending motions (Harvey & Cheung, 1977; Hvidt et al., 1982, 1984; Rosser et al., 1978; Highsmith, 1981).

The experiments described here are the product of a reinvestigation of the electrooptical properties of HMM and S1. S1 contains the MgATP and actin binding sites. HMM

† This research was supported by grants from the California Affiliate of the American Heart Association and from the National Institutes of Health (AM25177, GM31674, and Research Career Development Awards to S.H. and D.E.).

[1] Abbreviations: HMM, heavy meromyosin; S1, myosin subfragment 1; S2, myosin subfragment 2; LMM, light meromyosin; LC, light chain; Tris, tris(hydroxymethyl)aminomethane; EDTA, ethylenediaminetetraacetic acid; K_{sp}, specific birefringence; Δn, birefringence; SDS, sodium dodecyl sulfate.

0006-2960/85/0424-4917$01.50/0

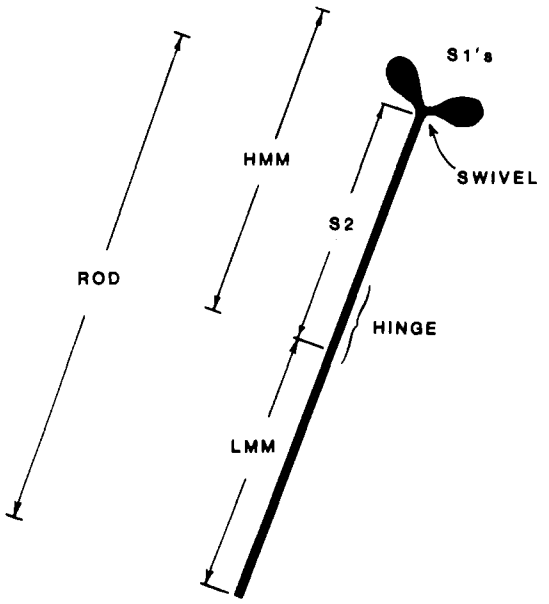

FIGURE 1: Myosin. Two elongated globular portions (S1's) are attached by a flexible swivel to a long coiled-coil of α-helixes that can bend at the hinge region near the center. Each S1 portion has two smaller proteins, called light chains, bound to it noncovalently. The rod, subfragment 2 (S2), light meromyosin (LMM), and heavy meromyosin (HMM) fragments are indicated.

consists of two S1's attached to the same end of the long coiled coil of α-helixes. Several reasons warrant a reinvestigation of HMM and S1 using electrical birefringence. The preparations of S1 and HMM and their characterizations have been improved since the original study by Kobayasi & Totsuka (1975). Electrooptical instrumentation has also been improved. The use of laser light and computer averaging of the signal has improved the time resolution and made the method nondestructive to proteins. Also, the previous demonstrations of swivel flexibility have utilized probes, and those results should be quantitatively confirmed by a method that does not depend on a probe for its signal. In addition, there are recent data suggesting that S1 itself may display segmental motions (Yagi, 1975; Balint et al., 1975; Mornet et al., 1979; Highsmith et al., 1979). Because birefringence decay reports motions from all the protein structure and is uncomplicated by possible uncertainties in probe orientation or local mobility, it is potentially a very useful method for analyzing S1 segmental motions. Finally, having accurate information of the specific birefringence of HMM and S1 in solution, which comprise the moving parts of the contractile apparatus of muscle, will help one interpret changes in birefringence that are observed for muscle fibers, where mechanical work can occur.

Experimental Procedures

Proteins and Chemicals. Myosin was prepared by the method of Nauss et al. (1969) and stored for up to 6 months at −20 °C. HMM and S1 were prepared from myosin by the procedures of Weeds & Pope (1977) with slight modification. In both cases, the weight ratio of α-chymotrypsin (Sigma) to myosin was 1 to 2500, and the reaction was quenched after 10 min. HMM prepared this way has light chains 1, 2, and 3 present (see Results for analysis). S1 prepared this way has only light chains 1 or 3 (Weeds & Pope, 1977). The S1 used in this study contained a mixture of light chains 1 and 3. Protein solutions were dialyzed to the required buffer and spun 1 h at 140000g before an electric birefringence measurement.

All chemicals were reagent grade or better. ATPase activities at 25 °C in 5 mM $CaCl_2$, 2 mM ATP, and 50 mM KCl were analyzed by using a phosphomolybdate method described by Murphy (1981). Analysis of protein molecular weights by gel electrophoresis in the presence of sodium dodecyl sulfate (SDS) was done according to Weber & Osborn (1969) using the polyacrylamide gel method described by Laemmli (1970) and markers of known molecular weights. Gels were stained with Coomassie Brilliant Blue R-250 and scanned at 555 nm by using a modified MacPherson Model EU 700 spectrophotometer. Areas under curves were determined gravimetrically.

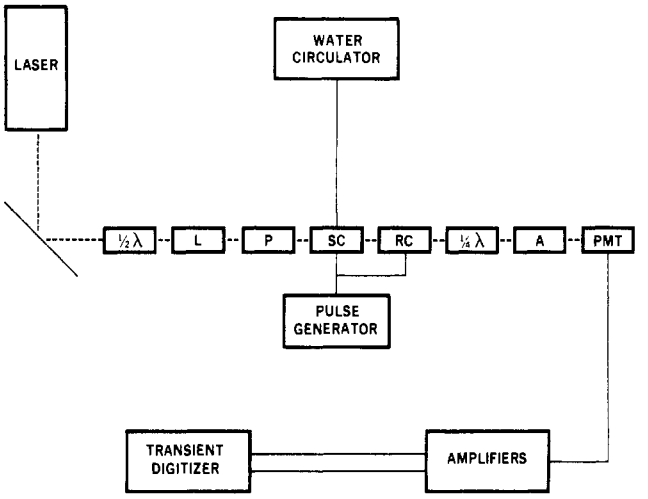

FIGURE 2: Transient electrical birefringence apparatus. The symbols in this schematic diagram are as follows: laser, Lexel Model 95 argon ion laser; $^1/_2\lambda$, half wave plate; L, lens; P and A, high-extinction Glan–Thompson polarizers; SC, sample cell; RC, reference cell; $^1/_4\lambda$, one-quarter wave plate; A, amplifiers (see text); PMT, RCA 4840 photomultipler tube; transient digitizer, le Croy 3500 with 100- and 32-MHz 8-bit digitizers; pulse generator, see text.

The length of the S2 portion of HMM was estimated by using eq 1. In this procedure, the molecular weight of the

$$\text{S2 length} = 2(M_r^{HMM} - M_r^{S1})(5.714 \times 10^{-4}\ \text{nm}) \quad (1)$$

heavy chain of HMM has the molecular weight of the heavy chain of S1 (95000; Weeds & Pope, 1977; Mornet et al., 1975) subtracted, and the difference is multiplied by 2 to obtain a molecular weight for S2 as part of HMM. This molecular weight is then multiplied by 5.714×10^{-4} nm which was obtained from the length and molecular weight of LMM (Lowey et al., 1969; Lowey, 1971; Highsmith et al., 1977). The validity of eq 1 is not easily demonstrated by using data from HMM because the length of S2 varies with the method of preparation (Harrington & Rodgers, 1984; Burke et al., 1973; Goodno et al., 1976; Highsmith et al., 1977; Lowey, 1971). However, when eq 1 is used for myosin to obtain a length for the myosin rod, M_r 230000 for the myosin heavy chain (Harrington & Rodgers, 1984), one obtains a length of 154 nm. This is in excellent agreement with the contour length of 156 nm obtained by Elliott & Offer (1978) from electron micrographs.

Instrumentation. The birefringence instrument (Figure 2) is an improved version of the one described by Elias & Eden (1981) and Eden & Elias (1983).

(*A*) *Optics.* The photomultiplier tube has been changed to an RCA 4840 in order to improve the quantum efficiency. With it and a 100-mW incident intensity at 514 nm, a photocurrent of 50 μA is obtained with an analyzer angle (β) of less than 0.3° from the crossed position. This results in a higher signal to noise ratio when the inverse extinction coefficient (K_{ex}^{-1}) of the polarizers is very high. It is important to know K_{ex}^{-1} for each experiment. It can be calculated simply

by noting that the background intensity doubles as β is varied from zero (the null) to a value such that $\sin^2 \beta = K_{ex}^{-1}$. Typical inverse extinction coefficients of 4×10^{-7} are an improvement over those obtained previously with the same polarizers. Weak focusing of the laser beam with a 50-cm focal length lens reduces the cross-section with which it interacts at the cell windows, a source of stress birefringence, and keeps the beam away from the electrode surfaces.

A reference Kerr cell has been inserted in the optical path between the sample cell and the one-quarter wave plate. This cell is used to optically cancel the buffer birefringence with no degradation of the signal to noise ratio. The electrode spacing of the reference cell has been machined to be exactly the same as that of the sample cell. Therefore, when an electrical signal is applied in parallel to the cells, the electric field across each cell will be identical. The reference cell has a length slightly longer than the sample cell, and it is mounted in a precision rotary device that permits adjustment of the field direction so that when it is filled with water its birefringence can canel the birefringence of the sample cell filled with buffer. This is important in the measurement of dilute solutions of small biopolymers which have small specific Kerr constants.

(*B*) *Electronics*. The study of the rotational diffusion constant of small macromolecules requires very fast electronics to capture the decay of the birefringence. The solutions have been excited with either a Velonex 360 high-power pulse generator or a Huggins 961D cable discharge pulser to provide 350-ns-wide pulses that have rise and decay times of less than 5 ns. A Keithley Model 104 wide-band amplifier provides an alternating current gain of 10 or 100 and a bandwidth in excess of 50 MHz for the signal from the photomultiplier. To determine the birefringence amplitude, the steady-state background light intensity (I_0) must be recorded. It is obtained by amplifying the output of the PMT with a Phillips Scientific 6931 DC-100 MHz amplifier. This amplifier is then followed by the Keithley amplifier and a step attenuator to adjust the amplitude to match the input characteristics of the LeCroy 3500 programmable averaging multichannel analyzer which contains Model TR8818/MM8103 and TR8837F transient recorders.

The overall system response has been evaluated by using a sample of low-salt buffer. It was subjected to 1000-V pulses from the Huggins pulser. The output of the LeCroy 3500 yields an overall system rise and fall time of 20 ns when the TR8818/MM8103 with its 10-ns sampling rate is used.

Calculations. The specific birefringence is determined by using (Elias & Eden, 1981)

$$K_{sp} = \Delta n / C_v 1.33 E^2 \quad (2)$$

where Δn is the solution birefringence, E is the electric field in statvolts per centimeter, C_v is the volume fraction of the sample, and 1.33 is the index of refraction of water at 4 °C. The volume fraction is obtained from a knowledge of its specific volume (typically 0.73 cm^3/g for proteins) and the weight fraction. The birefringence, Δn, is obtained from

$$\Delta n = (\lambda_0/\pi l)\{\beta - \arcsin[(\Delta I/I_0)(\sin^2 \beta + K_{ex}^{-1}) + \sin^2 \beta]^{1/2}\} \quad (3)$$

where ΔI is the change in intensity induced by the electric field, I_0 is the background intensity, λ_0 is the vacuum wavelength of the illuminating light (514 nm), l is the interaction length (2.9 cm), and β and K_{ex}^{-1} are as defined above.

The decay of the birefringence has been fit with a single exponential using a program run on the LeCroy data acquisition system. The background channels are selected either immediately proceding the applied pulse or many time constants after the field has been turned off. Linear regression is applied to the logarithm of the difference in the amplitude of the signal minus that of the background. Two-exponential fits were done by using a least-squares fitting procedure. Fits usually cover two to three time constants. The reported uncertainties reflect one standard deviation from an unweighted fit to the data.

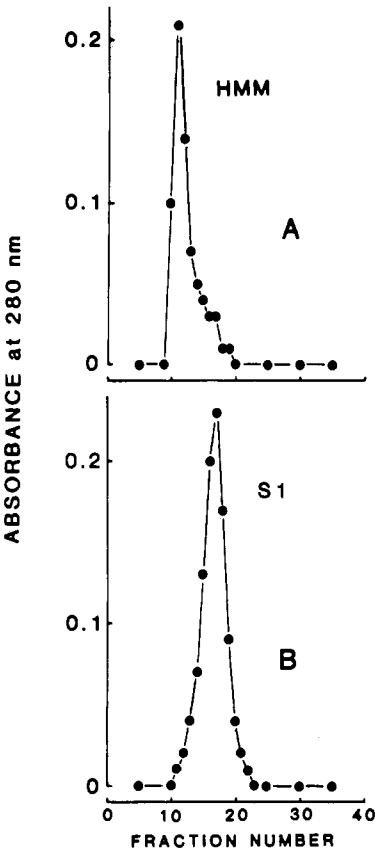

FIGURE 3: HMM and S1 purification. (A) After proteolysis of myosin and removal of unreacted myosin by centrifugation, the crude HMM was loaded on a 1.5 × 40 cm column filled with Sephacryl-S400 and eluted with 10 mM KCl, 5 mM Tris (pH 7.0), and 1 mM $MgCl_2$. Fractions of the eluent were collected, and the protein concentration was determined by the absorbance at 280 nm. The peak fraction only was used for experiments. (B) Same procedure as above, but for S1 in this case.

Results and Discussion

Characterization of Proteins. The HMM prepared from monomeric myosin by the action of α-chymotrypsin in the presence of 1 mM $MgCl_2$ was purified by size-exclusion chromatography. Panel A in Figure 3 shows a typical elution pattern. Five preparations were used for the birefringence measurements. Comparable data for S1 prepared from myosin filaments using α-chymotrypsin in the absence of $MgCl_2$ are shown in Figure 3B. The CaATPase activities in the presence of 6 μM $MgCl_2$ were 7.8 mol of P_i mol^{-1} s^{-1} for HMM and 3.0 mol of P_i mol^{-1} s^{-1} for S1. The HMM preparations were analyzed for light-chain and heavy-chain content by gel electrophoresis in the presence of SDS. The light chains were well resolved on 12% polyacrylamide gels (Figure 4A). The molar ratio of light chains, determined from the relative areas underneath the peaks obtained by scanning the Coomassie Brilliant Blue stained gels, was 1.0:1.9:0.90 for light chains 1, 2, and 3, respectively, when the results from three preparations were averaged. The corresponding ratios for myosin were 1.0:2.0:0.92, indicating that light chain 2 were damaged

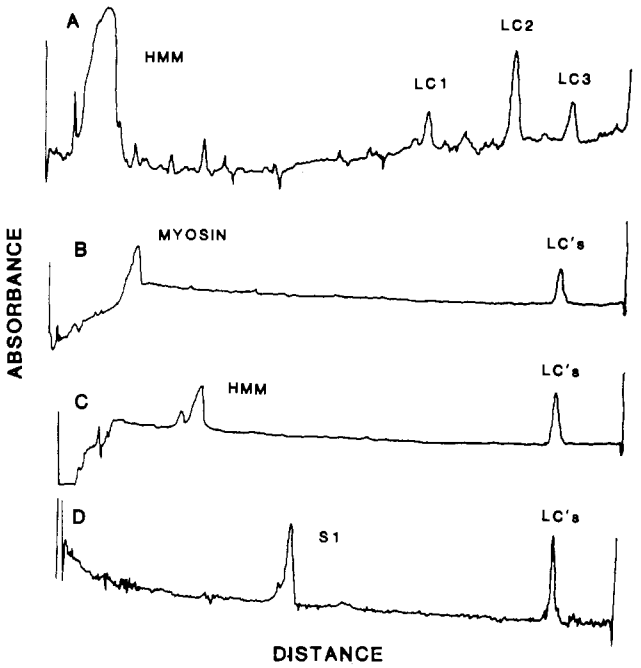

FIGURE 4: Gel electrophoresis. (A) HMM loaded and run on a 12% polyacrylamide gel. The gel was stained with Coomassie Brilliant Blue G-250 and scanned at 555 nm. The heavy-chain and light-chain components are well resolved. (B) Myosin on 7% polyacrylamide gels. (C) HMM on 7% gels. (D) S1 on 7% gels.

very little, if at all, in the HMM preparations. Thus, the often volatile light chain 2 is unperturbed by α-chymotrypsin at the low concentrations used. The HMM heavy chain appears on the 12% gels to be single band with M_r 155K, as determined from its mobility on the gels relative to the mobilities of proteins of known molecular weights. This molecular weight for HMM corresponds to a length of 69 nm (using eq 1) for the S2 portion and is consistent with data on preparation of the so-called "long" S2 (Sutoh et al., 1978; Goodno et al., 1976; Highsmith et al., 1977). It should be noticed that the gel scan in Figure 4A indicates less heavy-chain fragmentation in the 140K–75K range than usually observed in published scans of gels of HMM preparations, indicating that the reduced [α-chymotrypsin] spares the heavy chain, as well as light chain 2.

However, when the same HMM sample was analyzed by using 7% polyacrylamide gels that do not resolve the light chains, two heavy-chain components were observed, at M_r 145K and 168K, with a molar ratio of 3.3:1.0 (Figure 4C). Fragments of these molecular weights in these proportions were found reproducibly. Myosin and S1 heavy chains were homogeneous on 7% polyacrylamide gels (Figure 4B,D). The absence of excess or extra bands corresponding to M_r 23K in Figure 4A indicates that the two HMM heavy chains in Figure 4C are from HMM species with differing S2 lengths (see Figure 1) and not due to proteolysis of the S1 portion of HMM that is readily obtained with trypsin (Yagi, 1975; Mornet et al., 1979; Balint et al., 1975). The S2 lengths for the two HMM species using eq 1 are 56 and 82 nm.

Fast HMM Birefringence Decay Times. When solutions of HMM were subjected to a short pulse of an electric field (0.35–0.50 μs, 100–650 V/cm), the birefringence was positive, and the decay after the field was terminated was adequately described by a single exponential. The results were the same within experimental error, when obtained with a pulse generator or a cable discharge pulser. The average rotational relaxation time (τ in $\Delta n = \Delta n_{max} e^{-t/\tau}$) was 0.55 ± 0.021 μs at 4 °C. A typical trace of the changes in birefringence is

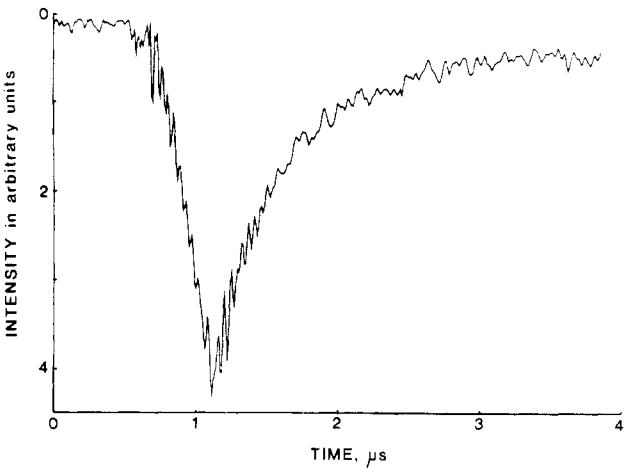

FIGURE 5: Fast decay of HMM birefringence. A solution of 0.54 μM HMM, 5 mM KCl, 5 mM Tris (pH 7 at 4 °C), 0.5 mM EDTA, and 1.5 mM $MgCl_2$ was subjected to 0.5-μs pulses of 600 V/cm at 200-ms intervals. The birefringence signal was collected for 100 pulses. The sampling interval was 0.010 μs, and full scale is 4.0 μs. The relaxation time at 4 °C for a single-exponential fit is 0.55 μs.

Table I: Relaxation Times for HMM and S1 Rotational Brownian Motion after Short Pulses of an Electric Field

sample	pulse length (μs)	τ^a
HMM	0.35–0.50	0.34
	120	0.7[b]
	0	0.32[c]
	0	0.24[d]
S1	0.35–0.50	0.13
	120	0.25[e]
	0	0.22[c]
	0	0.13[d]

[a] All data are adjusted to 20 °C; solution conditions as in Figure 5. [b] Obtained from a two-exponential fit to the decay curve after a 120-μs pulse (Kobayasi & Totsuka, 1975). [c] Results from saturation-transfer electron-spin resonance measurements (Thomas et al., 1975). [d] Results from time-resolved fluorescence anisotropy decay measurements (Mendelson et al., 1973). [e] Estimated from hand-smoothed traces of the birefringence decay after a 120-μs pulse (Kobayasi & Totsuka, 1975).

shown in Figure 5. The signal is tentatively assigned to the S1 portions of HMM. The possibility is remote that the HMM has unequal lengths of heavy chain in a single molecule and that the longer single strand of α-helix is the source of the observed signal. Single strands of naturally occurring α-helix in aqueous solution lack structural integrity and would likely fold up on themselves and be too small to give the observed relaxation time. Further evidence against this possibility is in the next section.

Most relaxation time data are scaled to 20 °C by adjusting for temperature–viscosity effects, for comparison to other results. The lack of any electrical birefringence detected phase change for myosin rod in the 0–43 °C range (Hvidt et al., 1984) justifies this procedure here. The fast relaxation time for HMM, adjusted to 20 °C, is 0.34 μs which is considerably faster than 0.7 μs, obtained previously from two-exponential fits to decay data for higher [HMM], at about 20 °C, which had been subjected to a much longer (120 μs) pulse (Kobayasi & Totsaka, 1975). However, the value reported here is consistent with the results obtained by using other methods (Table I). This consistency demonstrates the advantages of the improved instrumentation. It appears that with a short electric field pulse, the S1 portion of HMM can be selectively perturbed and its hydrodynamic return to equilibrium in the absence of the field is resolved and can be monitored directly. The fact that the birefringence relaxes to a base line slightly

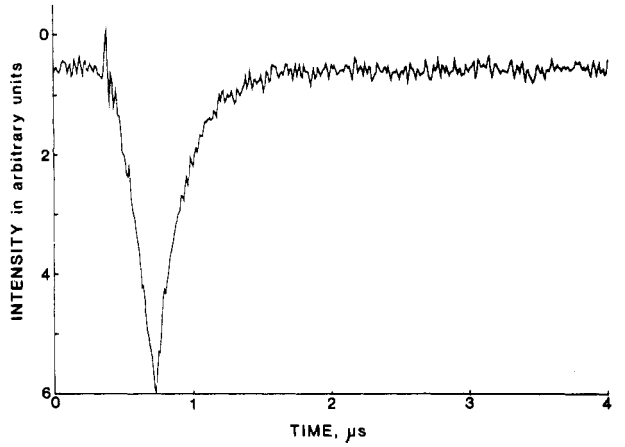

FIGURE 6: Decay of S1 birefringence. A solution of 0.26 μM S1, 5 mM KCl, 5 mM Tris (pH 7 at 4 °C), 0.5 mM EDTA, and 1.5 mM $MgCl_2$ was subjected to 0.35-μs pulses of 650 V/cm at 500-μs intervals. The rise and decay of the electrical birefringence result from 1000 pulses. The sampling interval was 0.010 μs. The relaxation time at 4 °C for a single-exponential fit was 0.21 μs.

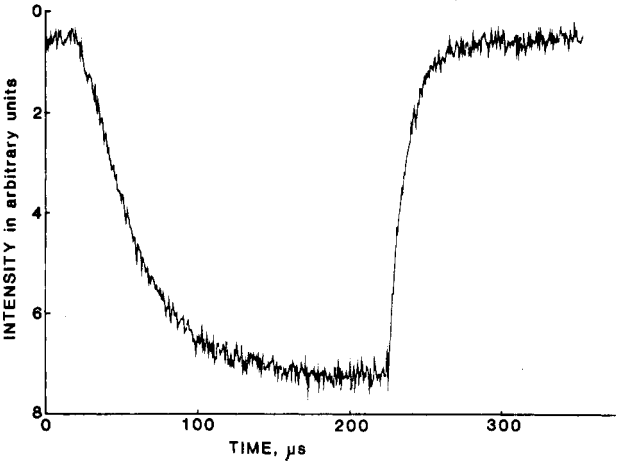

FIGURE 7: HMM steady-state birefringence. The sample is the same as in Figure 5. The pulse was 200 μs long and 150 V/cm. A total of 100 pulses were recorded. The sampling interval was 0.64 μs. The relaxation time at 4 °C for a single exponential fit was 13.6 μs.

below the starting base line indicates that some of the S2 portion is being oriented during this short pulse but that there is not a significant decay of orientation during the short time required for the S1 portion to randomize. The CaATPase activity after the short pulse measurements was at least 92% of the original value. If the sample was subjected to longer pulses (>20 μs) and then short pulse measurements were performed, the fast decay time was unchanged, within experimental error, but the CaATPase activity was lost.

S1 Birefringence Decay Times. To strengthen the assignment of the fast decay times obtained from HMM to motions of the S1 portion, measurements were made on isolated S1. The time dependence of the rise and fall of the birefringence is shown in Figure 6. The CaATPase activity of S1 was unchanged, within experimental error, by these measurements. The average relaxation time for measurements on six S1 preparations was 0.21 ± 0.03 μs at 4 °C. This value for free S1 rotational Brownian motion is consistent with that predicted from the fast decay time observed for HMM, assuming that the S1 portions are attached by a free swivel (Belford et al., 1972; Wegener, 1982), and with the values obtained from measurements on S1 for similar conditions using fluorescent and spin-label probes (Mendelson et al., 1973; Thomas et al., 1975). Adjusted to 20 °C, $\gamma = 0.13$ μs, which is significantly smaller than the 0.25 μs estimated from the original electrical birefringence measurements (Kobayasi & Totsuka, 1975).

The length of S1 was estimated from the rotational relaxation time and that for a sphere of the same volume ($\tau_s = 80.4$ ns at 4 °C). Assuming that there is 0.30 g of water per gram of protein and that the observed relaxation time is due predominately to rotation around the minor axis and using the Perrin shape factor for a prolate ellipsoid (Cantor & Schimmel, 1980), the length is 16.6 nm. This length is consistent with values for hydrated S1 obtained from hydrodynamic measurements (Mendelson et al., 1973; Garrios et al., 1983) but shorter than those obtained from recent analyses of electron micrographs (Elliot & Offer, 1978; Takahashi, 1978).

The relaxation times for S1 and HMM are summarized and compared to existing data in Table I. Wegener (1982) has used the ratio of the relaxation time of S1 in HMM to S1 free to characterize the degree of flexibility in the swivel region of myosin. For a freely moving prolate ellipsoidal S1 attached to the S2 portion, the ratio is expected to be in the range of 1.7–1.9. The ratio obtained here is 2.6. This suggests that the S1 motion is restricted, that S1 is not well described as a prolate ellipsoid, or that the S2 portion of HMM is making a significant contribution to the fast decay observed for HMM. The third possibility is unlikely in light of the data in Figures 5 and 6, which indicate the slow component of HMM relaxation is much smaller than and well-resolved from the fast component. The second possibility is feasible. Hydrodynamic data for S1 are perhaps fit better by an oblate ellipsoid than a prolate elliposid (Yang & Wu, 1977), and the best shape that fits electron-scattering data is far from prolate (Kretzschmar et al., 1978; Mendelson & Kretzschmar, 1980). The first possibility is also feasible. The rotation of free S1 about its minor axis corresponds to rotational motions of the attached S1 about the axis that is perpendicular to the major axis of the S2 protion of HMM. In both cases, this is the slowest rotational mode and the major contributor to the observed relaxation times. The irregular real shape of free S1 probably makes contributions to the observed relaxation times for rotations about axes other than the minor axis. Attached to HMM, the corresponding motion would be torsional rotation of S1 about the major axis of the S2 portion. If torsional motions were restricted, the ratio of relaxation times would be higher than expected for unrestricted motion. Such a restriction of torsional motion could have the functional significance in muscle of keeping S1 properly oriented with respect to the thin filament.

Slow HMM Birefringence Relaxation Time. When the duration of the electric field pulse was increased, a much larger birefrigence signal was observed which decayed with a longer relaxation time back to the original base line. The rise of the birefringence to its steady state and its decay are shown in Figure 7. The dependence of the amplitude of the birefringence signal on the strength of the applied electric field was well described by Kerr's law (Figure 8). The relaxation of the birefringence from steady-state values was 13.6 ± 0.5 μs at 4 °C when fit to a single-exponential decay. Adjusted to 20 °C, $\tau = 8.3$ μs, which is in reasonable agreement with the value of 8.9 μs obtained by Bernengo & Cardinand (1982) for HMM in solutions at much higher ionic strength.

Because the gels show the HMM is bidisperse, the decay data in Figure 6 were compared to the two-exponential expression

$$\Delta n/\Delta n_{max} = a \exp(-t/\tau_1) + b \exp(-t/\tau_2) \quad (4)$$

The preexponential terms were derived from the relative

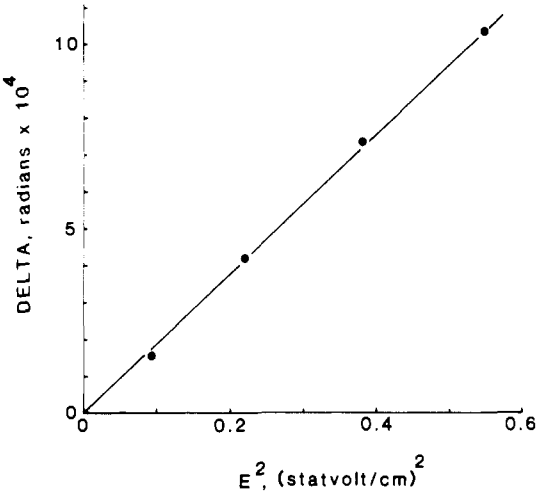

FIGURE 8: Kerr plot for HMM. The steady-state retardation, $\delta = 2\pi l\Delta n/\lambda_0$, is plotted as a function of the square of the electrical field for 0.41 mg/mL HMM in solution as described in Figure 5. The pulse length was 200 μs. The distance between the electrodes was 0.27 cm.

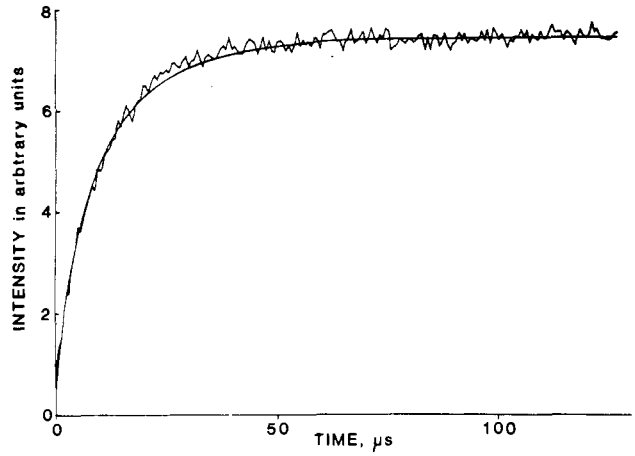

FIGURE 9: Slow decay of HMM birefringence. The data for the decay shown in Figure 7 are plotted with the curve predicted (see text for explanation) for HMM with rigid straight S2 portions.

amounts of the two HMM components and their respective lengths as follows:

$$a = 3.3(56\text{ nm})^2/[3.3(56\text{ nm})^2 + (82\text{ nm})^2] \quad (5)$$

and

$$b = (82\text{ nm})^2/[3.3(56\text{ nm})^2 + (82\text{ nm})^2] \quad (6)$$

where the birefringence was taken as proportional to the square of the length (Mellado & Garcia de la Torre, 1982) of S2 for the contributions from the smaller and larger components and weighted by the relative amounts determined by gel electrophoresis. Values of 0.61 and 0.39 were obtained for a and b, respectively, by using eq 5 and 6. Relaxation times of τ_1 = 5.2 μs and τ_2 = 16.1 μs were determined from the lengths for S2 by using the analysis of Garcia de la Torre & Bloomfield (1980) which assumes a straight rigid S2 attached by a flexible linkage to the S1's. The decay data are not precise enough to accurately obtain values for four variable parameters. When the τ values were fixed at 5.2 and 16.1 μs and the preexponentials were allowed to vary, the best fit gave a = 0.44 and b = 0.56 (Figure 9). This is in reasonably good agreement with the calculated values and suggests that the assumptions made were valid. This does not exclude S2 being flexible and/or bent. However, the data are adequately fit by a model of HMM with a S1's attached by flexible joints to a straight

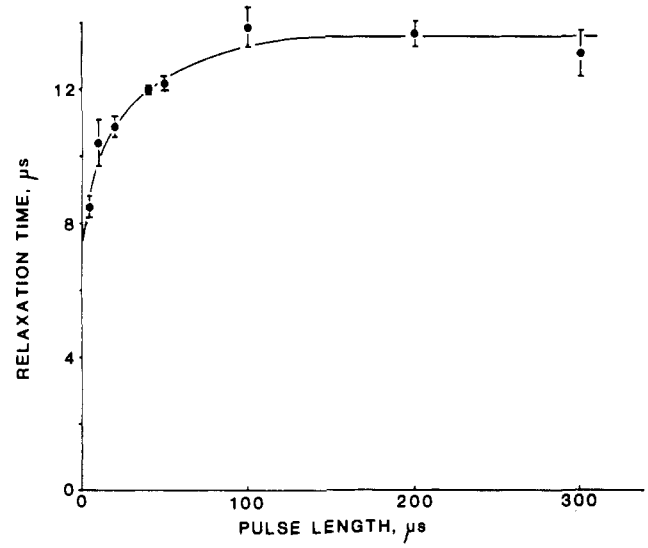

FIGURE 10: Pulse length dependence of HMM slow relaxation time. The relaxation time, τ, for the HMM is plotted for pulse lengths between 5 and 200 μs. The field strength was 200 V/cm. The conditions are the same as given in Figure 5.

and rigid S2 portion. A more elaborate model is not justified at this time.

When the duration of the electric field pulse was reduced so that a steady-state birefringence signal was not obtained, the relaxation times obtained from single-exponential fits decreased. Data for pulses as short as 5 μs are shown in Figure 10. The value obtained by extrapolating to 0-μs pulse length is 7.5 μs. This relaxation time dependence on pulse length is consistent with the heterogeneity of HMM.

Specific Birefringence of S1 and HMM. The specific birefringence for S1 was $(0.37 \pm 0.18) \times 10^{-6}$ (cm/statvolt)^2. This compares favorably with the value of $(0.5\text{–}2.0) \times 10^{-6}$ (cm/statvolt)^2 obtained by Kobayasi & Totsuka (1975). The value obtained for HMM was $(12.8 \pm 0.9) \times 10^{-6}$ (cm/statvolt)^2 when measurements were made by using alternating pulse polarity. If alternating pulse polarity was not used, the apparent K_{sp} for HMM was lower by as much as a factor of 10 after several measurements had been made. Protein concentration determinations indicated a loss of HMM from the solution, suggesting that without the alternating pulse polarity the HMM migrated during the experiment to one of the electrodes. The value obtained for HMM is close to 11×10^{-6} (cm/statvolt)^2, obtained by using a single-pulse method (Kobayasi & Totsuka, 1975), and larger than 5.7×10^{-6} (cm/statvolt)^2, obtained by using a signal-averaging method (Bernengo & Cardinand, 1982). The value for K_{sp}^{HMM}/K_{sp}^{S1} is 35, indicating that the birefringence signal from HMM will dominate the signal obtained from cross bridge movement in muscle fibers.

CONCLUSIONS

HMM is a popular myosin fragment for biochemical studies because it is soluble but retains the two-headedness of myosin. The preparation in this study has improved ratios of light-chain components, which are identical with those of myosin, within experimental error. This is relevant to the investigation of HMM segmental motions because it appears that the light chains are close to or part of the swivel region (Flicker et al., 1981; Craig et al., 1980). The apparent homogeneity of the HMM heavy chain on 12% polyacrylamide gels, which are widely used to analyze light-chain and heavy-chain composition for HMM preparations, is potentially misleading. The data for 7% polyacrylamide gels show there are two components;

7% polyacrylamide gels are usually not run for HMM because the light chains are not resolved (Figure 4), but these results suggest they should be run routinely. The smaller HMM heavy chain does not appear to result from proteolysis of the S1 portion, so the heterogeneity would not have been detected in biochemical studies, but the heavy-chain heterogeneity must be addressed in HMM hydrodynamic studies. Homogeneous heavy-chain distribution along with proper light-chain distribution was never obtained for reasons unclear to us.

The CaATPase activities of the HMM and S1 were adequate. Short pulses of electric fields did not reduce the activities significantly. This has not been demonstrated in earlier electrical birefringence studies of S1, HMM, or myosin (Kobayasi & Totsuka, 1975; Bernengo & Cardinand, 1982; Hvidt et al., 1984). Longer pulses destroyed the activity without changing the hydrodynamic properties, suggesting the loss of activity due to a subtle change in structure caused by the field or transient heating due to the electric field. The temperature was monitored continuously during a measurement from a thermistor imbedded in the sample cell, and heating was never observed.

The fast relaxation times for HMM and the corresponding S1 data confirm the results obtained with methods using probes (see Table I) and strongly indicate that the fast motion observed here for HMM is due to its S1 portions. The instrumentation can resolve rotational motions with relaxation times greater than 20 ns. The relaxation time obtained for S1 is in good agreement with existing data (Table I). Thus, the probe-free study of the hydrodynamics of native and modified S1's is possible by this method. We have demonstrated that small proteins, such as S1, can be analyzed by electrical birefringence decay techniques. The high ratio of attached to free S1 relaxation times suggests that a mode of rotation available to free S1 may be absent for S1 in HMM.

The slow relaxation times observed for HMM are undoubtedly due to the S2 portion of HMM, on the basis of the size of the signal ($K_{sp}^{HMM} = 35K_{sp}^{S1}$) and the agreement of the τ values observed with those predicted from theory (Garcia de la Torre & Bloomfield, 1982). The results shown in Figure 10 are consistent with both the larger and smaller HMM's having straight rigid S2 portions, in which case the flexibility of the myosin rod (Highsmith et al., 1977, 1982; Bernengo & Cardinaux, 1982; Hvidt et al., 1982; Roser et al., 1978) would be localized at the hinge region that is susceptible to proteolysis.

ACKNOWLEDGMENTS

It is a pleasure to thank Stella Ling for excellent technical assistance, Matheen Haleem for developing some of the computer programs used, and Professor F. Carlson for a critical reading of the manuscript.

REFERENCES

Balint, M., Streter, F. A., & Gergely, J. (1975) *Arch. Biochem. Biophys. 168*, 557–566.

Belford, G., Belford, R., & Weber, G. (1972) *Proc. Natl. Acad. Sci. U.S.A. 69*, 1392–1397.

Bernengo, J., & Cardinand, R. (1982) *J. Mol. Biol. 15*, 501–517.

Burke, M., Himmelfarb, S., & Harrington, W. F. (1973) *Biochemistry 12*, 701–710.

Cantor, C. R., & Schimmel, P. R. (1980) in *Biophysical Chemistry*, pp 560–565, W. H. Freeman, San Francisco, CA.

Craig, R., Szent-Gyorgyi, A. G., Besse, L., Flicker, P., Vibert, P., & Cohen, C. (1980) *J. Mol. Biol. 140*, 35–55.

Eden, D., & Elias, J. G. (1983) in *Measurement of Suspended Particles by Quasi-elastic Light Scattering* (Dahneke, B., Ed.) Wiley, New York.

Elias, J. G., & Eden, D. (1981) *Macromolecules 14*, 410–419.

Elliot, A., & Offer, G. (1978) *J. Mol. Biol. 123*, 505–519.

Flicker, P., Walliman, T., & Vibert, P. (1981) *Biophys. J. 33*, 279a.

Garcia de la Torre, J., & Bloomfield, V. (1980) *Biochemistry 19*, 5118–5123.

Garrigos, M., Morel, J. E., & Garcia de la Torre, J. (1983) *Biochemistry 22*, 4961–4969.

Gergely, J. (1950) *Fed. Proc., Fed. Am. Soc. Exp. Biol. 9*, 176.

Goodno, C., Harris, T., & Swenson, C. (1976) *Biochemistry 15*, 5157–5160.

Harrington, W. F., & Rodgers, M. E. (1984) *Annu. Rev. Biochem. 53*, 35–73.

Harvey, S., & Cheung, H. (1977) *Biochemistry 16*, 5181–5187.

Highsmith, S. (1981) *Biochim. Biophys. Acta 639*, 31–39.

Highsmith, S., Kretzschmar, M. K., O'Konski, C., & Morales, M. F. (1977) *Proc. Natl. Acad. Sci. U.S.A. 74*, 4986–4990.

Highsmith, S., Akasaka, K., Konrad, M., Goody, R., Holmes, K., Wade-Jardetzky, N., & Jardetzky, O. (1979) *Biochemistry 18*, 4238–4244.

Highsmith, S., Wang, C., Zero, K., Pecora, R., & Jardetzky, O. (1982) *Biochemistry 21*, 1192–1197.

Huxley, A. F., & Simmons, R. (1971) *Nature (London) 233*, 533–538.

Huxley, H. E. (1969) *Science (Washington, D.C.) 164*, 1355–1356.

Hvidt, S., Nestler, F., Greaser, M., & Ferry, J. (1982) *Biochemistry 21*, 4064–4073.

Hvidt, S., Chang, T., & Yu, H. (1984) *Biopolymers 23*, 1283–1294.

King, M. (1976) *Experientia 32*, 975–976.

Kobayasi, S., & Totsuka, T. (1975) *Biochim. Biophys. Acta 376*, 375–385.

Kretschmar, K. M., Mendelson, R. A., & Morales, M. F. (1978) *Biochemistry 17*, 2314–2318.

Laemmli, U. (1970) *Nature (London) 227*, 680–685.

Lowey, S. (1971) in *Subunits in Biological Systems, Part A* (Timasheff, S. N., & Fasman, G. D., Eds.) pp 201–259, Marcel Dekker, New York.

Lowey, S., Slayter, H., Weeds, A., & Baker, H. (1969) *J. Mol. Biol. 42*, 1–69.

Mellado, P., & Garcia de la Torre, J. (1982) *Biopolymers 21*, 1857–1871.

Mendelson, R. A., & Kretschmar, K. M. (1980) *Biochemistry 19*, 4103–4108.

Mendelson, R. A., Morales, M., & Botts, J. (1973) *Biochemistry 12*, 2250–2255.

Mornet, D., Pantel, P., Audemard, E., & Kassab, R. (1979) *Biochem. Biophys. Res. Commun. 89*, 925–932.

Murphy, A. J. (1981) *J. Biol. Chem. 256*, 12046–12050.

Nauss, K., Kitagawa, S., & Gergely, J. (1969) *J. Biol. Chem. 244*, 755–765.

Rosser, R., Nestler, F., Schrag, J., Ferry, J., & Greaser, M. (1978) *Macromolecules 11*, 1239–1242.

Slater, H., & Lowey, S. (1967) *Proc. Natl. Acad. Sci. U.S.A. 58*, 1611–1619.

Sutoh, K., Karr, T., & Harrington, W. (1978) *J. Mol. Biol. 126*, 1–22.

Szent-Gyorgyi, A. (1953) *Arch. Biochem. Biophys. 42*, 308–320.

Takahashi, K. (1978) *J. Biochem. (Tokyo) 83*, 905–908.
Thomas, D., Seidel, J., Hyde, J., & Gergely, J. (1975) *Proc. Natl. Acad. Sci. U.S.A. 72*, 1729–1733.
Weber, K., & Osborn, M. (1969) *J. Biol. Chem. 244*, 4406–4416.
Weeds, A., & Pope, B. (1977) *J. Mol. Biol. 111*, 129–157.
Wegener, W. A. (1982) *Biopolymers 21*, 1049–1080.
Yagi, K. (1975) *Adv. Biophys. 8*, 1–34.
Yang, J. T., & Wu, C. S. C. (1977) *Biochemistry 16*, 5785–5789.

Cross-Linking of the Anticodon of P and A Site Bound tRNAs to the Ribosome via Aromatic Azides of Variable Length: Involvement of 16S rRNA at the A Site

Piotr Gornicki,[‡] Jerzy Ciesiolka, and James Ofengand*
Roche Institute of Molecular Biology, Roche Research Center, Nutley, New Jersey 07110
Received January 15, 1985

ABSTRACT: The topography of the ribosomal decoding site was explored by affinity labeling from the 5′-anticodon base, 5-(carboxymethoxy)uridine-34, of P or A site bound $tRNA_1^{Val}$. A nitrophenyl azide was attached to the carboxyl group of this nucleotide via side chains varying in length from 18 to 24 Å. Binding of acetylvalyl-tRNA to the P site was codon dependent and that of valyl-tRNA to the A site was both codon and elongation factor Tu (EFTu) dependent. Cross-linking to both A and P sites was irradiation, probe, codon, and, in the case of the A site, EFTu dependent. Putative P-site cross-linked aminoacyl-tRNA was reactive with puromycin. The yield of cross-linking was little affected by placement of the tRNA at the A or P site but varied considerably with the length and structure of the probe side chain. When the distance from the pyrimidine C-5 atom to the azide group was 23 Å, 42–45% cross-linking was obtained at each site, but when the distance was decreased to 18 Å, only 7–12% was found. Placing an S–S bond in the center of the 23-Å leash decreased the A-site yield to about half, while insertion of a CONH group decreased A-site cross-linking about 8-fold. P-site cross-linking was more sensitive to mercaptan quenching (50% at 0.5 mM) than was that at the A site (50% at >2.0 mM) but both were partially shielded from solvent. A-site cross-linking was mainly (≥60%) to the 16S rRNA with the remainder being to 30S protein(s). P-site cross-linking was only to 30S proteins. However, as the P-site cross-link was not completely stable to isolation, there may also be unstable cross-linking elsewhere. Sequence analysis of the cross-linked oligomer(s) is described by Ciesiolka et al. [Ciesiolka, J., Gornicki, P., & Ofengand, J. (1985) *Biochemistry* (following paper in this issue)].

Previous studies from this laboratory have shown that the anticodon loop of tRNA bound at the ribosomal P site can be cross-linked by cyclobutane dimer formation to a specific single-stranded loop of 16S rRNA (Ofengand et al., 1979; Ofengand & Liou, 1980). Cross-linking is between the 5′-anticodon base, 5-(carboxymethoxy)uridine-34 (cmo^5U-34)[1] in $tRNA_1^{Val}$, the tRNA used for most of these experiments, and C-1400 of 16S RNA (Prince et al., 1982; Ehresmann et al., 1984). Analogous cross-linking has been found in yeast (Ofengand et al., 1982; Ehresmann et al., 1984) and *Artemia salina* (Ciesiolka et al., 1985b) ribosomes to a cytidine residue which is the eukaryotic equivalent of C-1400. This cytidine is located in the center of a 16 nucleotide long sequence that has been conserved in all known small subunit rRNA primary structures [reviewed in Ofengand et al. (1984)]. The significance of this close association between P-site tRNA anticodon and 16S rRNA is so far not known, although the conservation of both sequence and proximity to the anticodon across all species studied is a strong indication of functional importance.

The involvement of rRNA at the decoding site indicated by these findings prompted us to ask what other segments of 16S RNA might also be involved. Although the secondary structure of this RNA is now well established (Noller, 1984; Brimacombe et al., 1983), its tertiary folding in the ribosome is little understood and the only functions so far known for 16S RNA are the well-established Shine–Dalgarno base-pairing interaction with mRNA [reviewed by Gold et al. (1981)] and the anticodon decoding site contact at C-1400 cited above. In order to locate additional regions of rRNA near the decoding site without the limitation of chemical or photochemical requirements for cross-linking, as in cyclobutane dimer formation, a nonspecific aryl azide photoaffinity probe was attached to the same tRNA nucleotide, cmo^5U-34. The

[‡] Present address: Institute of Bioorganic Chemistry, Polish Academy of Sciences, Noskowskiego 12/14 61-704, Poznan, Poland.

[1] Abbreviations: EFTu, elongation factor Tu from *Escherichia coli*; cmo^5U-34, 5-(carboxymethoxy)uridine at position 34 of tRNA; NAK, 6-[(2-nitro-4-azidophenyl)amino]caproate; SuNOH, *N*-hydroxysuccinimide; NAK–SuNO, SuNOH ester of NAK; NAG, (2-nitro-4-azidophenyl)glycine; NAG–SuNO, SuNOH ester of NAG; NAL, *N*-(NAG)-β-alanine; NAL–SuNO, SuNOH ester of NAL; SNAP, 3-[[2-[(4-azido-2-nitrophenyl)amino]ethyl]dithio]propionate; SNAP–SuNO, the SuNOH ester of SNAP; EDC, 1-[3-(dimethylamino)-propyl]-3-ethylcarbodiimide; EDA, ethylenediamine; BD-cellulose, benzoylated DEAE-cellulose; Val-tRNA, valyl-tRNA; AcVal-tRNA; *N*-acetylvalyl-tRNA; $tRNA^{NAK}$ or $tRNA^{NAG}$, $tRNA^{Val}$ modified to contain a NAK or NAG group on the cmo^5U-34 residue as shown in Figure 1 of this paper; $tRNA^{SNAP}$ or $tRNA^{NAL}$, $tRNA^{Val}$ similarly modified to contain an NAL or SNAP group; Me_2SO, dimethyl sulfoxide; DNP, 2,4-dinitrophenyl; Hepes, *N*-(2-hydroxyethyl)piperazine-*N*′-2-ethanesulfonic acid; Mes, 2-(*N*-morpholino)ethanesulfonic acid; SDS, sodium dodecyl sulfate; PAGE, polyacrylamide gel electrophoresis; RNase, ribonuclease; TCA, trichloroacetic acid.

0006-2960/85/0424-4924$01.50/0